

Version 2.0.0 - SPARC: Simulation Package for Ab-initio Real-space Calculations

Boqin Zhang^a, Xin Jing^a, Qimen Xu^a, Shashikant Kumar^a, Abhiraj Sharma^c, Lucas Erlandson^b, Sushree Jagriti Sahoo^a, Edmond Chow^b, Andrew J. Medford^a, John E. Pask^c, Phanish Suryanarayana^{a,b,*}

^a*College of Engineering, Georgia Institute of Technology, Atlanta, GA 30332, USA*

^b*College of Computing, Georgia Institute of Technology, Atlanta, GA 30332, USA*

^c*Physics Division, Lawrence Livermore National Laboratory, Livermore, CA 94550, USA*

Abstract

SPARC is an accurate, efficient, and scalable real-space electronic structure code for performing ab initio Kohn-Sham density functional theory calculations. Version 2.0.0 of the software provides increased efficiency, and includes spin-orbit coupling, dispersion interactions, and advanced semilocal as well as hybrid exchange-correlation functionals, where it outperforms state-of-the-art planewave codes by an order of magnitude and more, with increasing advantages as the number of processors is increased. These new features further expand the range of physical applications amenable to first principles investigation.

Keywords: Kohn–Sham Density Functional Theory, Electronic structure, Relativistic effects, Dispersion interactions, Meta-GGA exchange-correlation, Hybrid exchange-correlation

Metadata

C1	Current code version	v2.0.0
C2	Permanent link to code/repository used for this code version	https://github.com/SPARC-X/SPARC/releases/tag/v2.0.0
C3	Permanent link to Reproducible Capsule	N/A
C4	Legal Code License	GNU General Public License v3.0
C5	Code versioning system used	Git
C6	Software code languages, tools, and services used	C, make, Python (for tests)
C7	Compilation requirements, operating environments & dependencies	Unix, Linux or MacOS; MPI, BLAS, LAPACK, ScaLAPACK (optional), MKL (optional), FFTW (optional)
C8	If available Link to developer documentation/manual	https://github.com/SPARC-X/SPARC/tree/master/doc
C9	Support email for questions	phanish.s@gmail.com

*corresponding author

Email address: phanish.suryanarayana@ce.gatech.edu (Phanish Suryanarayana)

1. Introduction

Over the past two decades, Kohn-Sham density functional theory (DFT) [1, 2] has established itself as one of the cornerstones of materials and chemical sciences research. However, Kohn-Sham calculations are associated with significant computational cost, scaling cubically with system size, severely limiting the length and time scales accessible to such a rigorous first principles investigation. The planewave pseudopotential method [3] has been among the most widely used techniques for the solution of the Kohn-Sham problem [4–11]. However, it is limited to periodic boundary conditions due to the underlying Fourier basis, whose global nature also hampers scalability on parallel computing platforms. This has motivated the development of alternative approaches employing systematically improvable, localized representations [12–33], with finite-difference methods perhaps the most mature and widely used to date.

SPARC [34] is a real-space electronic structure code for performing Kohn-Sham DFT calculations, where all quantities of interest, such as densities, potentials, and wavefunctions, are discretized on a uniform grid using the finite-difference approximation, enabling systematic control of convergence with a single parameter. It can accommodate both Dirichlet and Bloch-periodic boundary conditions, enabling the accurate and efficient treatment of finite, semi-infinite, and bulk 3D systems. SPARC has been extensively validated and benchmarked against established planewave codes. In particular, SPARC is able to efficiently leverage moderate and large-scale computational resources alike, efficiently scaling to thousands of processors in regular operation, and demonstrating order-of-magnitude speedups in time to solution relative to state-of-the-art planewave codes, with increasing advantages as the number of processors is increased.

2. Description of the software update

SPARC is designed to be portable and straightforward to install, use, and modify. In particular, external dependencies are limited to industry standard BLAS, LAPACK/ScaLAPACK, and MPI. It can perform spin-unpolarized as well as spin-polarized calculations, i.e., with fixed cell and ionic positions; geometry optimizations with respect to atom positions and/or cell; and ab initio molecular dynamics (AIMD) simulations, all using norm-conserving pseudopotentials [35, 36] with a range of local exchange-correlation functionals. Version 2.0.0 further expands the range of physical applications amenable to first principles investigation by further increasing efficiency and including spin-orbit coupling, dispersion interactions, and advanced semilocal as well as hybrid exchange-correlation functionals beyond the generalized gradient approximation (GGA) [3], as described below.

- Spin-orbit coupling (SOC): SOC refers to the relativistic electromagnetic interaction between the electron’s spin and orbital angular momenta [3]. SOC becomes more important as the atomic number increases, having a significant impact on the spectra of systems with heavy atoms. SOC has been implemented in SPARC through relativistic norm-conserving pseudopotentials [37], using the real-space formalism presented in Ref. [38].
- Dispersion interactions: The van der Waals (vdW) dispersion interaction, which is a correlation effect, represents the coupling between different parts of the system due to electronic charge fluctuations [3]. This long-range interaction becomes increasingly important in molecular and layered systems. Dispersion interactions have been implemented in SPARC through

the pairwise DFT-D3 correction [39] and the nonlocal vdW density functional (vdW-DF) [40, 41], for which we adopt the method presented in Refs. [42, 43].

- Meta-GGA exchange-correlation functionals: Residing on the third rung of Jacob's ladder [44], one rung above GGA, meta-GGA exchange-correlation functionals include a semilocal term that is dependent on the kinetic energy density, in addition to terms that are dependent on the electron density and its gradient which form the basis of GGA [3]. meta-GGA is implemented in SPARC through the recently developed SCAN functional, which satisfies all seventeen of the constraints known on the universal exchange-correlation functional [45].
- Hybrid exchange-correlation functionals: Residing on the fourth rung of Jacob's ladder, one rung above meta-GGA, hybrid functionals include a fraction of the nonlocal Hartree-Fock exact exchange energy, in addition to the terms found in meta-GGA and GGA. Hybrid functionals have been implemented in SPARC through the PBE0 [46] and HSE [47] functionals, using the methods presented in Refs. [48–50] for evaluating the exact exchange contribution.

In addition to the above functionalities, nonlinear core corrections (NLCC) — in which nonlinearity in the exchange-correlation functional is taken into account within the pseudopotential formalism — have been implemented; an extensive automated testing framework that includes examples with a wide range of system compositions, configurations, and dimensionalities has been developed; the SPMS table of pseudopotentials [51] — accurate, transferable, and soft optimized norm-conserving Vanderbilt (ONCV) pseudopotentials [35] with NLCC — has been incorporated into the distribution; and the overall implementation has been refined: optimized application of boundary conditions during stencil operations, optimized input parameters for the dense eigensolvers in ScaLAPACK, improved defaults for parallelization in the presence of Brillouin zone integration, and reformulation of the energy as well as forces to enable faster convergence within the self-consistent iteration, to further increase efficiency and parallel scaling.

In Fig. 1, we demonstrate the accuracy of the major new functionalities in SPARC through representative examples. In particular, we compare against the established planewave codes ABINIT v7.6.2 [52] and Quantum Espresso (QE) v7.1 [7]. Unless otherwise specified, we perform static calculations using ONCV pseudopotentials from the SPMS set and a 12th-order finite difference approximation for discretization. To demonstrate the accuracy of SPARC, we consider the following systems: (i) 4-atom cell of face-centered cubic (fcc) gold with PBE exchange-correlation, SOC using the relativistic ONCV pseudopotential from the PseudoDOJO set [53], $10 \times 10 \times 10$ grid for Brillouin zone integration, and real-space grid spacing of 0.15 bohr; (ii) fullerene molecule with PBE exchange-correlation, dispersion interactions through DFT-D3, and real-space grid spacing of 0.24 bohr; (iii) two 12-atom (3,3) carbon nanotubes with vdW-DF exchange-correlation, 10 grid points for Brillouin zone integration, and real-space grid spacing of 0.15 bohr; (iv) 14-atom cell of bulk Ni(CO₂)₂ with SCAN meta-GGA exchange-correlation, ONCV pseudopotentials without NLCC distributed with the ONCVPSP pseudopotential generation code [54] (SPARC v2.0.0 and the chosen versions of ABINIT as well as QE do not support SCAN with NLCC), 2 \times 2 \times 2 grid for Brillouin zone integration, and real-space grid spacing of 0.15 bohr; and (v) 24-atom cell of TiO₂ with HSE hybrid exchange-correlation, 6 \times 6 grid for Brillouin zone integration, and real-space grid spacing of 0.25 bohr. As shown in Fig. 1, SPARC shows excellent agreement with ABINIT as well as QE, where agreement can be increased as desired by refining the real-space grid.

Next, we demonstrate the efficiency and scaling of SPARC v2.0.0 through representative examples, as shown in Fig. 2. For new features, we compare against the state-of-the-art parallel

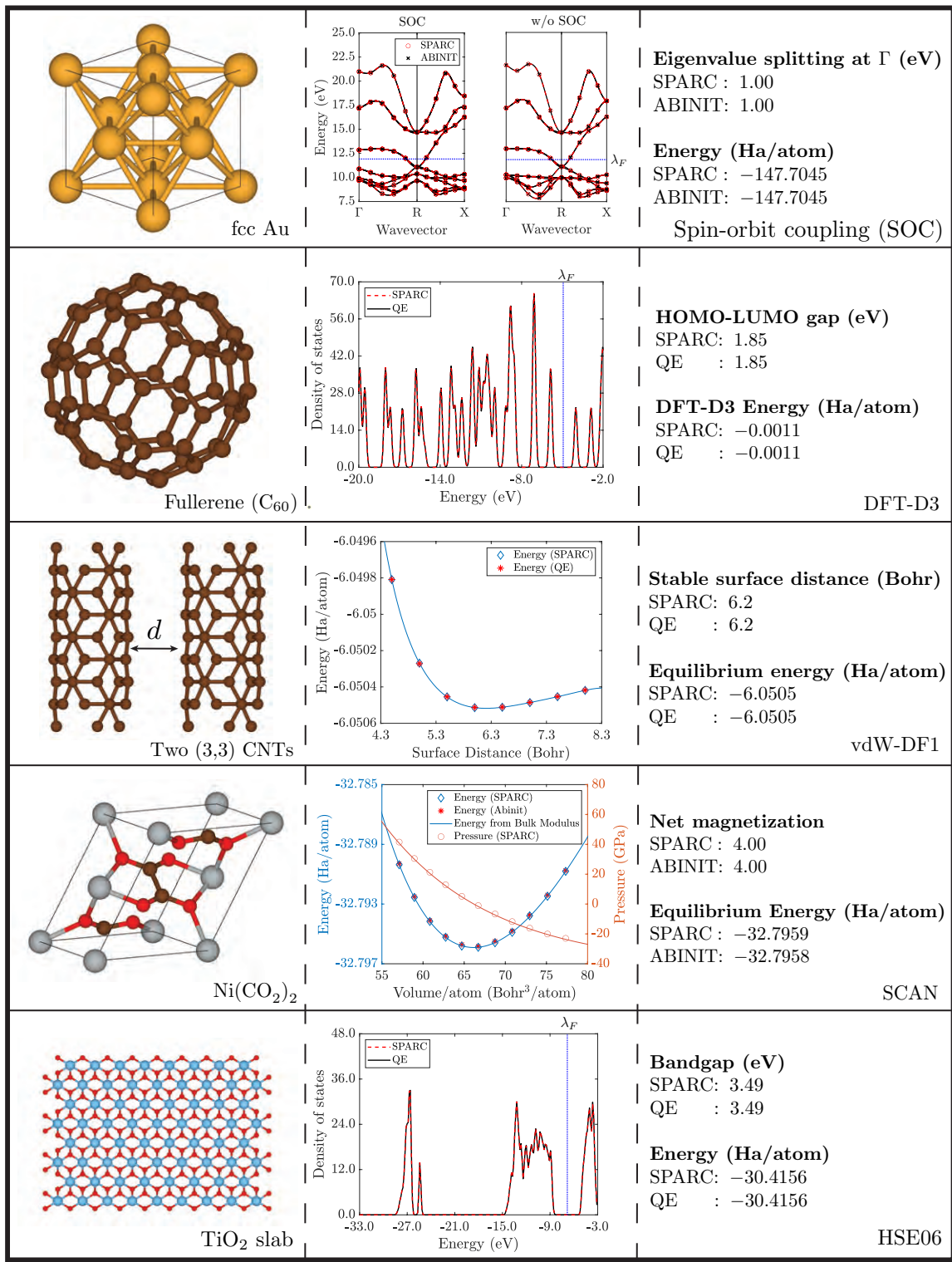


Figure 1: Examples demonstrating the accuracy of the new features in SPARC v2.0.0.

<ul style="list-style-type: none"> Systems: Bi_{32} and Cs_{29} slabs; Al_{256} and C_{216} bulk. Exchange-correlation: PBE. Brillouin zone integration: 4×4 grid (Bi_{32} and Cs_{29}); Γ-point (Al_{256} and C_{216}). Type of calculation: Static with force calculation. Discretization: 0.34 Bohr (Bi_{32}), 0.42 Bohr (Cs_{29}), 0.40 Bohr (Al_{256}), 0.25 Bohr (C_{216}). Accuracy: $\sim 1 \times 10^{-4}$ Ha/atom in energy. 	<ul style="list-style-type: none"> Systems: Al_{500} (1120 K), C_{512} (315.8 K), Al_{1372} (1120 K) and He_{2000} (2400 K). Exchange-correlation: PBE. Brillouin zone integration: Γ-point. Type of calculation: AIMD step. Timestep: 1 fs (Al_{500}, Al_{1372}), 1.5 fs (C_{512}) and 0.2 fs (He_{2000}). Discretization: 0.66 Bohr (Al_{500}, Al_{1372}) and 0.3 Bohr (C_{512}, He_{2000}). Accuracy: $\sim 1 \times 10^{-3}$ Ha/Bohr in force. 	<ul style="list-style-type: none"> Systems: Au_{72} wire, C_{254} bilayer graphene, $(\text{NiC}_2\text{O}_4)_{54}$ bulk and $(\text{TiO}_2)_{32}$ slab. C_{254} and $(\text{NiC}_2\text{O}_4)_{54}$ have two vacancies. Exchange-correlation: PBE (Au_{72}), vdW-DF1 (C_{254}), SCAN ($(\text{NiC}_2\text{O}_4)_{54}$), HSE06 ($(\text{TiO}_2)_{32}$). Brillouin zone integration: 4 grid points (Au_{72}); Γ-point (C_{254}, $(\text{NiC}_2\text{O}_4)_{54}$); 2×2 grid points ($(\text{TiO}_2)_{32}$). Type of calculation: Static with force calculation. Spin-polarized (C_{254}, $(\text{NiC}_2\text{O}_4)_{54}$). Discretization: 0.25 Bohr (Au_{72}, $(\text{TiO}_2)_{32}$), 0.29 Bohr (C_{254}), 0.24 Bohr ($(\text{NiC}_2\text{O}_4)_{54}$) in SPARC; 40 Ha ($\text{Au}_{72}$, C_{254}, $(\text{TiO}_2)_{32}$), 50 Ha ($(\text{NiC}_2\text{O}_4)_{54}$) in QE. Accuracy: $\sim 1 \times 10^{-4}$ Ha/atom in energy. 																																																																					
<table border="1"> <thead> <tr> <th colspan="3">Bi_{32}</th> </tr> <tr> <th>#cores</th> <th colspan="2">wall time (s)</th> </tr> <tr> <th></th> <th>v1.0</th> <th>v2.0</th> </tr> </thead> <tbody> <tr> <td>96</td> <td>388.4</td> <td>188.3</td> </tr> <tr> <td>192</td> <td>199.2</td> <td>88.8</td> </tr> <tr> <td>384</td> <td>109.2</td> <td>47.7</td> </tr> <tr> <td>768</td> <td>63.6</td> <td>35.5</td> </tr> <tr> <td>1200</td> <td>36.2</td> <td>18.6</td> </tr> </tbody> </table>	Bi_{32}			#cores	wall time (s)			v1.0	v2.0	96	388.4	188.3	192	199.2	88.8	384	109.2	47.7	768	63.6	35.5	1200	36.2	18.6	<table border="1"> <thead> <tr> <th colspan="3">Al_{500}</th> </tr> <tr> <th>#cores</th> <th colspan="2">wall time (s)</th> </tr> <tr> <th></th> <th>v1.0</th> <th>v2.0</th> </tr> </thead> <tbody> <tr> <td>30</td> <td>23.6</td> <td>9.2</td> </tr> <tr> <td>150</td> <td>8.5</td> <td>2.4</td> </tr> <tr> <td>450</td> <td>4.6</td> <td>1.5</td> </tr> <tr> <td>900</td> <td>4.5</td> <td>1.6</td> </tr> </tbody> </table>	Al_{500}			#cores	wall time (s)			v1.0	v2.0	30	23.6	9.2	150	8.5	2.4	450	4.6	1.5	900	4.5	1.6	<table border="1"> <thead> <tr> <th colspan="3">Au_{72} (SOC)</th> </tr> <tr> <th>#cores</th> <th colspan="2">wall time (s)</th> </tr> <tr> <th></th> <th>QE</th> <th>SPARC</th> </tr> </thead> <tbody> <tr> <td>240</td> <td>6876.5</td> <td>1521.6</td> </tr> <tr> <td>480</td> <td>4741.4</td> <td>778.0</td> </tr> <tr> <td>600</td> <td>4064.0</td> <td>720.2</td> </tr> <tr> <td>960</td> <td>3225.4</td> <td>444.8</td> </tr> <tr> <td>1920</td> <td>—</td> <td>286.8</td> </tr> </tbody> </table>	Au_{72} (SOC)			#cores	wall time (s)			QE	SPARC	240	6876.5	1521.6	480	4741.4	778.0	600	4064.0	720.2	960	3225.4	444.8	1920	—	286.8
Bi_{32}																																																																							
#cores	wall time (s)																																																																						
	v1.0	v2.0																																																																					
96	388.4	188.3																																																																					
192	199.2	88.8																																																																					
384	109.2	47.7																																																																					
768	63.6	35.5																																																																					
1200	36.2	18.6																																																																					
Al_{500}																																																																							
#cores	wall time (s)																																																																						
	v1.0	v2.0																																																																					
30	23.6	9.2																																																																					
150	8.5	2.4																																																																					
450	4.6	1.5																																																																					
900	4.5	1.6																																																																					
Au_{72} (SOC)																																																																							
#cores	wall time (s)																																																																						
	QE	SPARC																																																																					
240	6876.5	1521.6																																																																					
480	4741.4	778.0																																																																					
600	4064.0	720.2																																																																					
960	3225.4	444.8																																																																					
1920	—	286.8																																																																					
<table border="1"> <thead> <tr> <th colspan="3">Cs_{29}</th> </tr> <tr> <th>#cores</th> <th colspan="2">wall time (s)</th> </tr> <tr> <th></th> <th>v1.0</th> <th>v2.0</th> </tr> </thead> <tbody> <tr> <td>96</td> <td>248.4</td> <td>129.7</td> </tr> <tr> <td>192</td> <td>128.0</td> <td>71.0</td> </tr> <tr> <td>384</td> <td>72.1</td> <td>37.9</td> </tr> <tr> <td>768</td> <td>39.9</td> <td>20.3</td> </tr> <tr> <td>1200</td> <td>26.6</td> <td>23.5</td> </tr> </tbody> </table>	Cs_{29}			#cores	wall time (s)			v1.0	v2.0	96	248.4	129.7	192	128.0	71.0	384	72.1	37.9	768	39.9	20.3	1200	26.6	23.5	<table border="1"> <thead> <tr> <th colspan="3">C_{512}</th> </tr> <tr> <th>#cores</th> <th colspan="2">wall time (s)</th> </tr> <tr> <th></th> <th>v1.0</th> <th>v2.0</th> </tr> </thead> <tbody> <tr> <td>80</td> <td>41.5</td> <td>25.0</td> </tr> <tr> <td>150</td> <td>26.5</td> <td>11.8</td> </tr> <tr> <td>300</td> <td>14.6</td> <td>7.2</td> </tr> <tr> <td>600</td> <td>11.2</td> <td>5.7</td> </tr> </tbody> </table>	C_{512}			#cores	wall time (s)			v1.0	v2.0	80	41.5	25.0	150	26.5	11.8	300	14.6	7.2	600	11.2	5.7	<table border="1"> <thead> <tr> <th colspan="3">C_{254} (vdW-DF1)</th> </tr> <tr> <th>#cores</th> <th colspan="2">wall time (s)</th> </tr> <tr> <th></th> <th>QE</th> <th>SPARC</th> </tr> </thead> <tbody> <tr> <td>240</td> <td>188.2</td> <td>120.9</td> </tr> <tr> <td>480</td> <td>238.3</td> <td>65.3</td> </tr> <tr> <td>600</td> <td>173.2</td> <td>58.8</td> </tr> <tr> <td>960</td> <td>—</td> <td>49.0</td> </tr> <tr> <td>1920</td> <td>—</td> <td>39.1</td> </tr> </tbody> </table>	C_{254} (vdW-DF1)			#cores	wall time (s)			QE	SPARC	240	188.2	120.9	480	238.3	65.3	600	173.2	58.8	960	—	49.0	1920	—	39.1
Cs_{29}																																																																							
#cores	wall time (s)																																																																						
	v1.0	v2.0																																																																					
96	248.4	129.7																																																																					
192	128.0	71.0																																																																					
384	72.1	37.9																																																																					
768	39.9	20.3																																																																					
1200	26.6	23.5																																																																					
C_{512}																																																																							
#cores	wall time (s)																																																																						
	v1.0	v2.0																																																																					
80	41.5	25.0																																																																					
150	26.5	11.8																																																																					
300	14.6	7.2																																																																					
600	11.2	5.7																																																																					
C_{254} (vdW-DF1)																																																																							
#cores	wall time (s)																																																																						
	QE	SPARC																																																																					
240	188.2	120.9																																																																					
480	238.3	65.3																																																																					
600	173.2	58.8																																																																					
960	—	49.0																																																																					
1920	—	39.1																																																																					
<table border="1"> <thead> <tr> <th colspan="3">Al_{256}</th> </tr> <tr> <th>#cores</th> <th colspan="2">wall time (s)</th> </tr> <tr> <th></th> <th>v1.0</th> <th>v2.0</th> </tr> </thead> <tbody> <tr> <td>48</td> <td>39.3</td> <td>25.8</td> </tr> <tr> <td>96</td> <td>22.1</td> <td>14.6</td> </tr> <tr> <td>192</td> <td>12.7</td> <td>11.1</td> </tr> <tr> <td>384</td> <td>8.1</td> <td>5.9</td> </tr> <tr> <td>768</td> <td>7.3</td> <td>3.6</td> </tr> </tbody> </table>	Al_{256}			#cores	wall time (s)			v1.0	v2.0	48	39.3	25.8	96	22.1	14.6	192	12.7	11.1	384	8.1	5.9	768	7.3	3.6	<table border="1"> <thead> <tr> <th colspan="3">Al_{1372}</th> </tr> <tr> <th>#cores</th> <th colspan="2">wall time (s)</th> </tr> <tr> <th></th> <th>v1.0</th> <th>v2.0</th> </tr> </thead> <tbody> <tr> <td>192</td> <td>38.0</td> <td>18.8</td> </tr> <tr> <td>312</td> <td>26.4</td> <td>13.5</td> </tr> <tr> <td>768</td> <td>14.6</td> <td>7.4</td> </tr> <tr> <td>1536</td> <td>12.0</td> <td>5.8</td> </tr> </tbody> </table>	Al_{1372}			#cores	wall time (s)			v1.0	v2.0	192	38.0	18.8	312	26.4	13.5	768	14.6	7.4	1536	12.0	5.8	<table border="1"> <thead> <tr> <th colspan="3">$(\text{NiC}_2\text{O}_4)_{54}$ (SCAN)</th> </tr> <tr> <th>#cores</th> <th colspan="2">wall time (s)</th> </tr> <tr> <th></th> <th>QE</th> <th>SPARC</th> </tr> </thead> <tbody> <tr> <td>240</td> <td>1452.5</td> <td>1389.1</td> </tr> <tr> <td>480</td> <td>1067.0</td> <td>797.4</td> </tr> <tr> <td>600</td> <td>727.5</td> <td>625.2</td> </tr> <tr> <td>960</td> <td>1063.2</td> <td>360.2</td> </tr> <tr> <td>1920</td> <td>—</td> <td>216.4</td> </tr> </tbody> </table>	$(\text{NiC}_2\text{O}_4)_{54}$ (SCAN)			#cores	wall time (s)			QE	SPARC	240	1452.5	1389.1	480	1067.0	797.4	600	727.5	625.2	960	1063.2	360.2	1920	—	216.4
Al_{256}																																																																							
#cores	wall time (s)																																																																						
	v1.0	v2.0																																																																					
48	39.3	25.8																																																																					
96	22.1	14.6																																																																					
192	12.7	11.1																																																																					
384	8.1	5.9																																																																					
768	7.3	3.6																																																																					
Al_{1372}																																																																							
#cores	wall time (s)																																																																						
	v1.0	v2.0																																																																					
192	38.0	18.8																																																																					
312	26.4	13.5																																																																					
768	14.6	7.4																																																																					
1536	12.0	5.8																																																																					
$(\text{NiC}_2\text{O}_4)_{54}$ (SCAN)																																																																							
#cores	wall time (s)																																																																						
	QE	SPARC																																																																					
240	1452.5	1389.1																																																																					
480	1067.0	797.4																																																																					
600	727.5	625.2																																																																					
960	1063.2	360.2																																																																					
1920	—	216.4																																																																					
<table border="1"> <thead> <tr> <th colspan="3">C_{216}</th> </tr> <tr> <th>#cores</th> <th colspan="2">wall time (s)</th> </tr> <tr> <th></th> <th>v1.0</th> <th>v2.0</th> </tr> </thead> <tbody> <tr> <td>48</td> <td>59.4</td> <td>43.3</td> </tr> <tr> <td>96</td> <td>34.8</td> <td>24.3</td> </tr> <tr> <td>192</td> <td>22.4</td> <td>17.3</td> </tr> <tr> <td>384</td> <td>11.9</td> <td>7.9</td> </tr> <tr> <td>768</td> <td>6.8</td> <td>5.4</td> </tr> </tbody> </table>	C_{216}			#cores	wall time (s)			v1.0	v2.0	48	59.4	43.3	96	34.8	24.3	192	22.4	17.3	384	11.9	7.9	768	6.8	5.4	<table border="1"> <thead> <tr> <th colspan="3">He_{2000}</th> </tr> <tr> <th>#cores</th> <th colspan="2">wall time (s)</th> </tr> <tr> <th></th> <th>v1.0</th> <th>v2.0</th> </tr> </thead> <tbody> <tr> <td>275</td> <td>60.0</td> <td>48.7</td> </tr> <tr> <td>550</td> <td>38.0</td> <td>29.6</td> </tr> <tr> <td>1100</td> <td>31.4</td> <td>27.5</td> </tr> <tr> <td>2200</td> <td>25.9</td> <td>22.6</td> </tr> </tbody> </table>	He_{2000}			#cores	wall time (s)			v1.0	v2.0	275	60.0	48.7	550	38.0	29.6	1100	31.4	27.5	2200	25.9	22.6	<table border="1"> <thead> <tr> <th colspan="3">$(\text{TiO}_2)_{32}$ (HSE06)</th> </tr> <tr> <th>#cores</th> <th colspan="2">wall time (s)</th> </tr> <tr> <th></th> <th>QE</th> <th>SPARC</th> </tr> </thead> <tbody> <tr> <td>240</td> <td>9443.5</td> <td>1411.4</td> </tr> <tr> <td>480</td> <td>8083.4</td> <td>725.6</td> </tr> <tr> <td>600</td> <td>8678.6</td> <td>611.9</td> </tr> <tr> <td>960</td> <td>—</td> <td>446.0</td> </tr> <tr> <td>1920</td> <td>—</td> <td>292.2</td> </tr> </tbody> </table>	$(\text{TiO}_2)_{32}$ (HSE06)			#cores	wall time (s)			QE	SPARC	240	9443.5	1411.4	480	8083.4	725.6	600	8678.6	611.9	960	—	446.0	1920	—	292.2
C_{216}																																																																							
#cores	wall time (s)																																																																						
	v1.0	v2.0																																																																					
48	59.4	43.3																																																																					
96	34.8	24.3																																																																					
192	22.4	17.3																																																																					
384	11.9	7.9																																																																					
768	6.8	5.4																																																																					
He_{2000}																																																																							
#cores	wall time (s)																																																																						
	v1.0	v2.0																																																																					
275	60.0	48.7																																																																					
550	38.0	29.6																																																																					
1100	31.4	27.5																																																																					
2200	25.9	22.6																																																																					
$(\text{TiO}_2)_{32}$ (HSE06)																																																																							
#cores	wall time (s)																																																																						
	QE	SPARC																																																																					
240	9443.5	1411.4																																																																					
480	8083.4	725.6																																																																					
600	8678.6	611.9																																																																					
960	—	446.0																																																																					
1920	—	292.2																																																																					

Figure 2: Examples demonstrating the performance of SPARC v2.0.0.

planewave code QE v7.1, whereas for previously implemented features, we compare against SPARC v1.0.0, which has already been benchmarked against QE in Ref. [34]. Unless otherwise specified, we use ONCV pseudopotentials from the SPMS set and a 12th-order finite difference approximation for discretization. We use a relativistic ONCV pseudopotential from the PseudoDOJO set for the SOC calculation, and ONCV pseudopotentials without NLCC distributed with the ONCVPSP pseudopotential generation code for the SCAN calculation. In both SPARC and QE, we use the default parallelization settings. All calculations are performed on the Phoenix cluster at Georgia Tech, comprised of Dual Intel Xeon Gold 6226 CPUs @ 2.7 GHz (24 cores/node), DDR4-2933 MHz DRAM, and Infiniband 100HDR interconnect. Additional details regarding the systems selected, which include a wide range of sizes, the type of calculation performed, and computational parameters chosen for this study are shown in Fig. 2, the raw data for which is provided in Ref. [55]. It can be seen that SPARC demonstrates up to an order-of-magnitude speedup in time to solution with respect to QE for the new features, with increasing advantages as the number of processors is increased. Notably, the largest speedup occurs for the hybrid functional, due mainly to the superior scalability of domain decomposition in real-space vs. planewave implementations. Furthermore, it can be seen that SPARC v2.0.0 is up to a factor of two faster than v1.0.0, which is itself an order of magnitude faster than QE [34].

3. Impact and future development

Kohn–Sham DFT calculations occupy a substantial fraction of the world’s high-performance computing resources every day [56, 57]. Since most of these calculations are performed using established planewave DFT codes [4–8, 11], any new code that consistently outperforms these state-of-the-art codes stands to have immediate and significant impact. The new functionalities in SPARC v2.0.0 allow for higher fidelity first principles simulations than possible with the previous version. Given that some of these features are computationally intensive, e.g., hybrid exchange-correlation functionals, the superior efficiency and scalability of SPARC relative to established planewave alternatives, demonstrating order of magnitude and more speedups, with increasing advantages as the number of processors is increased, stands to enable a number of physical applications that were previously beyond reach, as evidenced by recent publications employing SPARC [58–61].

Future releases of SPARC will include the following features, which while being under development in SPARC, have resulted in a number of publications [62–82]: the Discrete Discontinuous Basis Projection (DDBP) method [19], which brings down time to solution for large problems; GPU acceleration to bring down time to solution further still [62]; the linear scaling Spectral Quadrature (SQ) method [63, 83, 84], which has enabled system sizes as large as a million atoms [64] and has found a number of applications in warm dense matter [65–67]; cyclic+helical symmetry-adapted DFT [68, 69, 85], referred to as Cyclix-DFT [68], which has found a number of applications in the study of 1D and 2D nanomaterials subject to mechanical deformations [70–78]; real-space Density Functional Perturbation Theory (DFPT), which will enable the efficient calculation of the response to perturbations, e.g., phonons [86]; correlation energy within the Random Phase Approximation [3]; orbital-free DFT [79, 80], which has applications in the development of machine learning techniques [87, 88]; and on-the-fly machine-learned force-fields [81, 82], with the capability to treat many-element systems using the Gaussian multipole featurization scheme [89]. The development of such features is being accelerated by prototyping in the MATLAB version of SPARC, referred to as M-SPARC [90–92].

Acknowledgements

J.E.P., P.S., B.Z., and X.J. gratefully acknowledge support from U.S. Department of Energy (DOE), National Nuclear Security Administration (NNSA): Advanced Simulation and Computing (ASC) Program at LLNL. The authors also gratefully acknowledge support from grant DE-SC0019410 funded by the U.S. Department of Energy, Office of Science. This work was performed in part under the auspices of the U.S. Department of Energy by Lawrence Livermore National Laboratory under Contract DE-AC52-07NA27344.

References

- [1] W. Kohn, L. J. Sham, Self-consistent equations including exchange and correlation effects, *Physical Review* 140 (4A) (1965) A1133.
- [2] P. Hohenberg, W. Kohn, Inhomogeneous electron gas, *Physical Review* 136 (3B) (1964) 864.
- [3] R. M. Martin, Electronic structure: basic theory and practical methods, Cambridge University Press, 2020.
- [4] G. Kresse, J. Furthmüller, Efficient iterative schemes for ab initio total-energy calculations using a plane-wave basis set, *Physical Review B* 54 (16) (1996) 11169–11186.
- [5] S. J. Clark, M. D. Segall, C. J. Pickard, P. J. Hasnip, M. I. Probert, K. Refson, M. C. Payne, First principles methods using CASTEP, *Zeitschrift für Kristallographie-Crystalline Materials* 220 (5/6) (2005) 567–570.
- [6] X. Gonze, J. M. Beuken, R. Caracas, F. Detraux, M. Fuchs, G. M. Rignanese, L. Sindic, M. Verstraete, G. Zerah, F. Jollet, M. Torrent, A. Roy, M. Mikami, P. Ghosez, J. Y. Raty, D. C. Allan, First-principles computation of material properties: the ABINIT software project, *Computational Materials Science* 25 (2002) 478–492(15).
- [7] P. Giannozzi, S. Baroni, N. Bonini, M. Calandra, R. Car, C. Cavazzoni, D. Ceresoli, G. L. Chiarotti, M. Cococcioni, I. Dabo, A. D. Corso, S. de Gironcoli, S. Fabris, G. Fratesi, R. Gebauer, U. Gerstmann, C. Gougoussis, A. Kokalj, M. Lazzeri, L. Martin-Samos, N. Marzari, F. Mauri, R. Mazzarello, S. Paolini, A. Pasquarello, L. Paulatto, C. Sbraccia, S. Scandolo, G. Sclauzero, A. P. Seitsonen, A. Smogunov, P. Umari, R. M. Wentzcovitch, QUANTUM ESPRESSO: a modular and open-source software project for quantum simulations of materials, *Journal of Physics: Condensed Matter* 21 (39) (2009) 395502.
- [8] D. Marx, J. Hutter, Ab initio molecular dynamics: Theory and implementation, *Modern methods and algorithms of quantum chemistry* 1 (2000) 301–449.
- [9] S. Ismail-Beigi, T. A. Arias, New algebraic formulation of density functional calculation, *Computer Physics Communications* 128 (1-2) (2000) 1 – 45.
- [10] F. Gygi, Architecture of Qbox: A scalable first-principles molecular dynamics code, *IBM Journal of Research and Development* 52 (1.2) (2008) 137–144.

- [11] M. Valiev, E. Bylaska, N. Govind, K. Kowalski, T. Straatsma, H. V. Dam, D. Wang, J. Nieplocha, E. Apra, T. Windus, W. de Jong, NWChem: A comprehensive and scalable open-source solution for large scale molecular simulations, Computer Physics Communications 181 (9) (2010) 1477 – 1489.
- [12] A. D. Becke, Basis-set-free density-functional quantum chemistry, International Journal of Quantum Chemistry 36 (S23) (1989) 599–609.
- [13] J. R. Chelikowsky, N. Troullier, Y. Saad, Finite-difference-pseudopotential method: Electronic structure calculations without a basis, Physical Review Letters 72 (8) (1994) 1240–1243. doi: [10.1103/PhysRevLett.72.1240](https://doi.org/10.1103/PhysRevLett.72.1240).
- [14] L. Genovese, A. Neelov, S. Goedecker, T. Deutsch, S. A. Ghasemi, A. Willand, D. Caliste, O. Zilberberg, M. Rayson, A. Bergman, R. Schneider, Daubechies wavelets as a basis set for density functional pseudopotential calculations, The Journal of Chemical Physics 129 (1) (2008) 014109.
- [15] A. P. Seitsonen, M. J. Puska, R. M. Nieminen, Real-space electronic-structure calculations: Combination of the finite-difference and conjugate-gradient methods, Physical Review B 51 (20) (1995) 14057.
- [16] S. R. White, J. W. Wilkins, M. P. Teter, Finite-element method for electronic structure, Physical Review B 39 (9) (1989) 5819.
- [17] J.-I. Iwata, D. Takahashi, A. Oshiyama, T. Boku, K. Shiraishi, S. Okada, K. Yabana, A massively-parallel electronic-structure calculations based on real-space density functional theory, Journal of Computational Physics 229 (6) (2010) 2339–2363.
- [18] E. Tsuchida, M. Tsukada, Electronic-structure calculations based on the finite-element method, Physical Review B 52 (8) (1995) 5573.
- [19] Q. Xu, P. Suryanarayana, J. E. Pask, Discrete discontinuous basis projection method for large-scale electronic structure calculations, The Journal of Chemical Physics 149 (9) (2018) 094104.
- [20] P. Suryanarayana, K. Bhattacharya, M. Ortiz, A mesh-free convex approximation scheme for Kohn-Sham density functional theory, Journal of Computational Physics 230 (13) (2011) 5226 – 5238.
- [21] P. Suryanarayana, V. Gavini, T. Blesgen, K. Bhattacharya, M. Ortiz, Non-periodic finite-element formulation of Kohn-Sham density functional theory, Journal of the Mechanics and Physics of Solids 58 (2) (2010) 256 – 280.
- [22] C.-K. Skylaris, P. D. Haynes, A. A. Mostofi, M. C. Payne, Introducing ONETEP: Linear-scaling density functional simulations on parallel computers, The Journal of Chemical Physics 122 (8) (2005) 084119.
- [23] D. R. Bowler, R. Choudhury, M. J. Gillan, T. Miyazaki, Recent progress with large-scale ab initio calculations: the CONQUEST code, physica status solidi (b) 243 (5) (2006) 989–1000.

- [24] P. Motamarri, S. Das, S. Rudraraju, K. Ghosh, D. Davydov, V. Gavini, DFT-FE — A massively parallel adaptive finite-element code for large-scale density functional theory calculations, *Computer Physics Communications* 246 (2020) 106853.
- [25] A. Castro, H. Appel, M. Oliveira, C. A. Rozzi, X. Andrade, F. Lorenzen, M. A. L. Marques, E. K. U. Gross, A. Rubio, octopus: a tool for the application of time-dependent density functional theory, *Physica Status Solidi B-Basic Solid State Physics* 243 (11) (2006) 2465–2488.
- [26] E. L. Briggs, D. J. Sullivan, J. Bernholc, Real-space multigrid-based approach to large-scale electronic structure calculations, *Physical Review B* 54 (1996) 14362–14375.
- [27] J.-L. Fattebert, Finite difference schemes and block Rayleigh quotient iteration for electronic structure calculations on composite grids, *Journal of Computational Physics* 149 (1) (1999) 75 – 94.
- [28] F. Shimojo, R. K. Kalia, A. Nakano, P. Vashishta, Linear-scaling density-functional-theory calculations of electronic structure based on real-space grids: design, analysis, and scalability test of parallel algorithms, *Computer Physics Communications* 140 (3) (2001) 303 – 314.
- [29] S. Ghosh, P. Suryanarayana, SPARC: Accurate and efficient finite-difference formulation and parallel implementation of density functional theory: Isolated clusters, *Computer Physics Communications* 212 (2017) 189–204.
- [30] S. Ghosh, P. Suryanarayana, SPARC: Accurate and efficient finite-difference formulation and parallel implementation of density functional theory: Extended systems, *Computer Physics Communications* 216 (2017) 109–125.
- [31] T. A. Arias, Multiresolution analysis of electronic structure: semicardinal and wavelet bases, *Reviews of Modern Physics* 71 (1) (1999) 267–311.
- [32] J. E. Pask, P. A. Sterne, Finite element methods in ab initio electronic structure calculations, *Modelling and Simulation in Materials Science and Engineering* 13 (2005) R71–R96.
- [33] L. Lin, J. Lu, L. Ying, E. Weinan, Adaptive local basis set for Kohn–Sham density functional theory in a discontinuous Galerkin framework i: Total energy calculation, *Journal of Computational Physics* 231 (4) (2012) 2140–2154.
- [34] Q. Xu, A. Sharma, B. Comer, H. Huang, E. Chow, A. J. Medford, J. E. Pask, P. Suryanarayana, SPARC: Simulation package for ab-initio real-space calculations, *SoftwareX* 15 (2021) 100709.
- [35] D. Hamann, Optimized norm-conserving Vanderbilt pseudopotentials, *Physical Review B* 88 (8) (2013) 085117.
- [36] N. Troullier, J. L. Martins, Efficient pseudopotentials for plane-wave calculations, *Physical Review B* 43 (3) (1991) 1993.
- [37] L. Kleinman, Relativistic norm-conserving pseudopotential, *Physical Review B* 21 (6) (1980) 2630.

- [38] D. Naveh, L. Kronik, M. L. Tiago, J. R. Chelikowsky, Real-space pseudopotential method for spin-orbit coupling within density functional theory, *Physical Review B* 76 (15) (2007) 153407.
- [39] S. Grimme, J. Antony, S. Ehrlich, H. Krieg, A consistent and accurate ab initio parametrization of density functional dispersion correction (DFT-D) for the 94 elements H-Pu, *The Journal of Chemical Physics* 132 (15) (2010) 154104.
- [40] M. Dion, H. Rydberg, E. Schröder, D. C. Langreth, B. I. Lundqvist, Van der Waals density functional for general geometries, *Physical Review Letters* 92 (24) (2004) 246401.
- [41] K. Lee, É. D. Murray, L. Kong, B. I. Lundqvist, D. C. Langreth, Higher-accuracy van der Waals density functional, *Physical Review B* 82 (8) (2010) 081101.
- [42] G. Román-Pérez, J. M. Soler, Efficient implementation of a van der Waals density functional: application to double-wall carbon nanotubes, *Physical Review Letters* 103 (9) (2009) 096102.
- [43] T. Thonhauser, S. Zuluaga, C. Arter, K. Berland, E. Schröder, P. Hyldgaard, Spin signature of nonlocal correlation binding in metal-organic frameworks, *Physical Review Letters* 115 (13) (2015) 136402.
- [44] J. P. Perdew, K. Schmidt, Jacob's ladder of density functional approximations for the exchange-correlation energy, *AIP Conference Proceedings* 577 (2001) 1–20.
- [45] J. Sun, A. Ruzsinszky, J. P. Perdew, Strongly constrained and appropriately normed semilocal density functional, *Physical Review Letters* 115 (3) (2015) 036402.
- [46] C. Adamo, V. Barone, Toward reliable density functional methods without adjustable parameters: The PBE0 model, *The Journal of Chemical Physics* 110 (13) (1999) 6158–6170.
- [47] J. Heyd, G. E. Scuseria, M. Ernzerhof, Hybrid functionals based on a screened Coulomb potential, *The Journal of Chemical Physics* 118 (18) (2003) 8207–8215.
- [48] L. Lin, Adaptively compressed exchange operator, *Journal of Chemical Theory and Computation* 12 (5) (2016) 2242–2249.
- [49] J. Spencer, A. Alavi, Efficient calculation of the exact exchange energy in periodic systems using a truncated Coulomb potential, *Physical Review B* 77 (19) (2008) 193110.
- [50] F. Gygi, A. Baldereschi, Self-consistent Hartree-Fock and screened-exchange calculations in solids: Application to silicon, *Physical Review B* 34 (6) (1986) 4405.
- [51] M. F. Shojaei, J. E. Pask, A. J. Medford, P. Suryanarayana, Soft and transferable pseudopotentials from multi-objective optimization, *Computer Physics Communications* 283 (2023) 108594.
- [52] X. Gonze, B. Amadon, G. Antonius, F. Arnardi, L. Baguet, J.-M. Beuken, J. Bieder, F. Bottin, J. Bouchet, E. Bousquet, N. Brouwer, F. Bruneval, G. Brunin, T. Cavignac, J.-B. Charraud, W. Chen, M. Côté, S. Cottenier, J. Denier, G. Geneste, P. Ghosez, M. Giantomassi, Y. Gillet, O. Gingras, D. R. Hamann, G. Hautier, X. He, N. Helbig, N. Holzwarth, Y. Jia, F. Jollet, W. Lafargue-Dit-Hauret, K. Lejaeghere, M. A. Marques, A. Martin, C. Martins, H. P. Miranda, F. Naccarato, K. Persson, G. Petretto, V. Planes, Y. Pouillon, S. Prokhorenko, F. Ricci, G.-M.

- Rignanese, A. H. Romero, M. M. Schmitt, M. Torrent, M. J. van Setten, B. Van Troeye, M. J. Verstraete, G. Zérah, J. W. Zwanziger, The ABINIT project: Impact, environment and recent developments, Computer Physics Communications 248 (2020) 107042.
- [53] M. J. van Setten, M. Giantomassi, E. Bousquet, M. J. Verstraete, D. R. Hamann, X. Gonze, G.-M. Rignanese, The PseudoDojo: Training and grading a 85 element optimized norm-conserving pseudopotential table, Computer Physics Communications 226 (2018) 39–54.
- [54] D. R. Hamann, ONCVPPSP pseudopotential generation code, www.mat-simresearch.com, accessed: 2023-05-08.
- [55] B. Zhang, X. Jing, Q. Xu, S. Kumar, A. Sharma, L. Erlandson, S. J. Sahoo, E. Chow, A. J. Medford, J. E. Pask, P. Suryanarayana, Supporting Information for Version 2.0.0 - SPARC: Simulation Package for Ab-initio Real-space Calculations, Mendeley Data V1. doi:10.17632/mvsc6cznrm.1.
- [56] B. Austin, W. Bhimji, T. Butler, J. Deslippe, 2014 NERSC workload analysis, http://portal.nersc.gov/project/mpccc/baustin/NERSC_2014_Workload_Analysis_v1.1.pdf.
- [57] L. J. Vernon, IC Application Performance Team analysis, as part of IC Knights Special Project, Tech. Rep. LANL, 2015.
- [58] S. J. Sahoo, X. Jing, P. Suryanarayana, A. J. Medford, Ab-initio investigation of finite size effects in rutile titania nanoparticles with semilocal and nonlocal density functionals, The Journal of Physical Chemistry C 126 (4) (2022) 2121–2130.
- [59] S. J. Sahoo, Q. Xu, X. Lei, D. Staros, G. R. Iyer, B. Rubenstein, P. Suryanarayana, A. Medford, Self-consistent convolutional density functional approximations: Application to adsorption at metal surfaces, ChemPhysChem (2024) e202300688.
- [60] C. Zeng, S. J. Sahoo, A. J. Medford, A. A. Peterson, Phase stability of large-size nanoparticle alloy catalysts at ab initio quality using a nearsighted force-training approach, The Journal of Physical Chemistry C 127 (50) (2023) 24360–24372.
- [61] S. Pathrudkar, P. Thiagarajan, S. Agarwal, A. S. Banerjee, S. Ghosh, Electronic structure prediction of multi-million atom systems through uncertainty quantification enabled transfer learning, arXiv preprint arXiv:2308.13096.
- [62] A. Sharma, A. Metere, P. Suryanarayana, L. Erlandson, E. Chow, J. E. Pask, GPU acceleration of local and semilocal density functional calculations in the SPARC electronic structure code, The Journal of Chemical Physics 158 (20) (2023) 204117.
- [63] P. Suryanarayana, P. P. Pratapa, A. Sharma, J. E. Pask, SQDFT: Spectral Quadrature method for large-scale parallel O(N) Kohn–Sham calculations at high temperature, Computer Physics Communications 224 (2018) 288–298.
- [64] V. Gavini, S. Baroni, V. Blum, D. R. Bowler, A. Buccheri, J. R. Chelikowsky, S. Das, W. Dawson, P. Delugas, M. Dogan, C. Draxl, G. Galli, L. Genovese, P. Giannozzi, M. Giantomassi, X. Gonze, M. Govoni, F. Gygi, A. Gulans, J. M. Herbert, S. Kokott, T. D. Kühne, K.-H. Liou, T. Miyazaki, P. Motamarri, A. Nakata, J. E. Pask, C. Plessl, L. E. Ratcliff, R. M. Richard,

- M. Rossi, R. Schade, M. Scheffler, O. Schütt, P. Suryanarayana, M. Torrent, L. Truflandier, T. L. Windus, Q. Xu, V. W.-Z. Yu, D. Perez, Roadmap on electronic structure codes in the exascale era, *Modelling and Simulation in Materials Science and Engineering* 31 (6) (2023) 063301.
- [65] M. Bethkenhagen, A. Sharma, P. Suryanarayana, J. E. Pask, B. Sadigh, S. Hamel, Properties of carbon up to 10 million kelvin from Kohn-Sham density functional theory molecular dynamics, *Physical Review E* 107 (1) (2023) 015306.
- [66] S. Zhang, A. Lazicki, B. Militzer, L. H. Yang, K. Caspersen, J. A. Gaffney, M. W. Däne, J. E. Pask, W. R. Johnson, A. Sharma, P. Suryanarayana, D. D. Johnson, A. V. Smirnov, P. A. Sterne, D. Erskine, R. A. London, F. Coppapi, D. Swift, J. Nilsen, A. J. Nelson, H. D. Whitley, Equation of state of boron nitride combining computation, modeling, and experiment, *Physical Review B* 99 (16) (2019) 165103.
- [67] C. J. Wu, P. C. Myint, J. E. Pask, C. J. Prisbrey, A. A. Correa, P. Suryanarayana, J. B. Varley, Development of a multiphase beryllium equation of state and physics-based variations, *The Journal of Physical Chemistry A* 125 (7) (2021) 1610–1636.
- [68] A. Sharma, P. Suryanarayana, Real-space density functional theory adapted to cyclic and helical symmetry: Application to torsional deformation of carbon nanotubes, *Physical Review B* 103 (3) (2021) 035101.
- [69] S. Ghosh, A. S. Banerjee, P. Suryanarayana, Symmetry-adapted real-space density functional theory for cylindrical geometries: Application to large group-IV nanotubes, *Physical Review B* 100 (12) (2019) 125143.
- [70] S. Kumar, P. Suryanarayana, Bending moduli for forty-four select atomic monolayers from first principles, *Nanotechnology* 31 (43) (2020) 43LT01.
- [71] S. Kumar, P. Suryanarayana, On the bending of rectangular atomic monolayers along different directions: an ab initio study, *Nanotechnology* 34 (8) (2022) 085701.
- [72] D. Codony, I. Arias, P. Suryanarayana, Transversal flexoelectric coefficient for nanostructures at finite deformations from first principles, *Physical Review Materials* 5 (3) (2021) L030801.
- [73] S. Kumar, D. Codony, I. Arias, P. Suryanarayana, Flexoelectricity in atomic monolayers from first principles, *Nanoscale* 13 (3) (2021) 1600–1607.
- [74] A. Bhardwaj, P. Suryanarayana, Strain engineering of Janus transition metal dichalcogenide nanotubes: an ab initio study, *The European Physical Journal B* 95 (3) (2022) 59.
- [75] A. Bhardwaj, A. Sharma, P. Suryanarayana, Torsional strain engineering of transition metal dichalcogenide nanotubes: an ab initio study, *Nanotechnology* 32 (47) (2021) 47LT01.
- [76] A. Bhardwaj, A. Sharma, P. Suryanarayana, Torsional moduli of transition metal dichalcogenide nanotubes from first principles, *Nanotechnology* 32 (28) (2021) 28LT02.
- [77] A. Bhardwaj, P. Suryanarayana, Ab initio study on the electromechanical response of Janus transition metal dihalide nanotubes, *The European Physical Journal B* 96 (3) (2023) 36.

- [78] A. Bhardwaj, P. Suryanarayana, Elastic properties of Janus transition metal dichalcogenide nanotubes from first principles, *The European Physical Journal B* 95 (1) (2022) 13.
- [79] S. Ghosh, P. Suryanarayana, Higher-order finite-difference formulation of periodic orbital-free density functional theory, *Journal of Computational Physics* 307 (2016) 634–652.
- [80] P. Suryanarayana, D. Phanish, Augmented Lagrangian formulation of orbital-free density functional theory, *Journal of Computational Physics* 275 (2014) 524–538.
- [81] S. Kumar, X. Jing, J. E. Pask, A. J. Medford, P. Suryanarayana, Kohn–Sham accuracy from orbital-free density functional theory via Δ -machine learning, *The Journal of Chemical Physics* 159 (24).
- [82] S. Kumar, X. Jing, J. E. Pask, P. Suryanarayana, On-the-fly machine learned force fields for the study of warm dense matter: application to diffusion and viscosity of CH, arXiv preprint arXiv:2402.13450.
- [83] P. P. Pratapa, P. Suryanarayana, J. E. Pask, Spectral Quadrature method for accurate O(N) electronic structure calculations of metals and insulators, *Computer Physics Communications* 200 (2016) 96–107.
- [84] P. Suryanarayana, On spectral quadrature for linear-scaling density functional theory, *Chemical Physics Letters* 584 (2013) 182–187.
- [85] A. S. Banerjee, P. Suryanarayana, Cyclic density functional theory: A route to the first principles simulation of bending in nanostructures, *Journal of the Mechanics and Physics of Solids* 96 (2016) 605–631.
- [86] A. Sharma, P. Suryanarayana, Calculation of phonons in real-space density functional theory, *Physical Review E* 108 (4) (2023) 045302.
- [87] B. Thapa, X. Jing, J. E. Pask, P. Suryanarayana, I. I. Mazin, Assessing the source of error in the Thomas–Fermi–von Weizsäcker density functional, *The Journal of Chemical Physics* 158 (21).
- [88] S. Kumar, B. Sadigh, S. Zhu, P. Suryanarayana, S. Hamel, B. Gallagher, V. Bulatov, J. Klepeis, A. Samanta, Accurate parameterization of the kinetic energy functional for calculations using exact-exchange, *The Journal of Chemical Physics* 156 (2) (2022) 024107.
- [89] X. Lei, A. J. Medford, A universal framework for featurization of atomistic systems, *The Journal of Physical Chemistry Letters* 13 (34) (2022) 7911–7919.
- [90] B. Zhang, X. Jing, S. Kumar, P. Suryanarayana, Version 2.0.0-M-SPARC: Matlab-simulation package for ab-initio real-space calculations, *SoftwareX* 21 (2023) 101295.
- [91] Q. Xu, A. Sharma, P. Suryanarayana, M-SPARC: Matlab-simulation package for ab-initio real-space calculations, *SoftwareX* 11 (2020) 100423.
- [92] P.-W. Huang, N. Tian, T. Rajh, Y.-H. Liu, G. Innocenti, C. Sievers, A. J. Medford, M. C. Hatzell, Formation of carbon-induced nitrogen-centered radicals on titanium dioxide under illumination, *JACS Au* 3 (12) (2023) 3283–3289.